Chloride channels in stellate cells are essential for uniquely high secretion rates in neuropeptide-stimulated *Drosophila* diuresis

Pablo Cabrero[a,1], Selim Terhzaz[a,1], Michael F. Romero[b,c], Shireen A. Davies[a], Edward M. Blumenthal[d], and Julian A. T. Dow[a,2]

[a]Institute of Molecular, Cell and Systems Biology, College of Medical, Veterinary and Life Sciences, University of Glasgow, Glasgow G12 8QQ, United Kingdom; [b]Department of Physiology and Biomedical Engineering and [c]Division of Nephrology and Hypertension, Mayo Clinic College of Medicine, Rochester, MN 55905; and [d]Department of Biological Sciences, Marquette University, Milwaukee, WI 53201-1881

Edited by David L. Denlinger, Ohio State University, Columbus, OH, and approved August 18, 2014 (received for review July 5, 2014)

Epithelia frequently segregate transport processes to specific cell types, presumably for improved efficiency and control. The molecular players underlying this functional specialization are of particular interest. In *Drosophila*, the renal (Malpighian) tubule displays the highest per-cell transport rates known and has two main secretory cell types, principal and stellate. Electrogenic cation transport is known to reside in the principal cells, whereas stellate cells control the anion conductance, but by an as-yet-undefined route. Here, we resolve this issue by showing that a plasma membrane chloride channel, encoded by *ClC-a*, is exclusively expressed in the stellate cell and is required for *Drosophila* kinin-mediated induction of diuresis and chloride shunt conductance, evidenced by chloride ion movement through the stellate cells, leading to depolarization of the transepithelial potential. By contrast, *ClC-a* knockdown had no impact on resting secretion levels. Knockdown of a second *CLC* gene showing highly abundant expression in adult Malpighian tubules, *ClC-c*, did not impact depolarization of transepithelial potential after kinin stimulation. Therefore, the diuretic action of kinin in *Drosophila* can be explained by an increase in *ClC-a*–mediated chloride conductance, over and above a resting fluid transport level that relies on other (*ClC-a*–independent) mechanisms or routes. This key segregation of cation and anion transport could explain the extraordinary fluid transport rates displayed by some epithelia.

Epithelia provide essential barrier and vectorial transport capabilities intrinsic to the success of higher organisms. Depending on their roles and specializations, epithelia may be termed tight or leaky, based on their electrical conductance, which in turn depends on the patency of their paracellular spaces. Tight epithelia are thought to have a highly restricted paracellular route because of prominent tight junctions (septate junctions in insects), so constraining transepithelial fluxes to a transcellular route. Leaky epithelia, traditionally associated with high flux rates, lack such prominent tight junctions.

Insect renal (Malpighian) tubules move fluid at the highest rates observed in biology, and thus would seem to be ideal candidates for leaky epithelia. However, insect tubule cells are typically large and multinucleate or polyploid (large cell diameters minimize the junctional circumference per unit transporting membrane), and the cells are also surrounded by prominent septate junctions (1). Nonetheless, it has been argued that, in tubules of the dengue fever mosquito *Aedes aegypti*, the rapid neurohormonally controlled chloride shunt conductance is paracellular, caused by remodeling of the septate junctions with switch-like speed under the influence of diuretic peptides of the kinin family (2, 3).

Drosophila melanogaster is a member of one of the largest insect orders, the Diptera, and these tubules are distinguished by a prominent secondary cell type, the stellate cell. The powerful transgenic toolbox available for *Drosophila* allows cell-specific contributions to tissue-level function to be probed; by expressing the luminescent calcium reporter apoaequorin transgenically in specific cell types, it was possible to show that kinin signals specifically through intracellular calcium in only the stellate cells (4)—and not the principal cells—consistent with the observed expression of the kinin receptor in just stellate cells (5). The biogenic amine tyramine also acts similarly; that is, it stimulates fluid secretion by activating a chloride shunt conductance by raising intracellular calcium levels in the stellate cells (6, 7). Thus—at least in *Drosophila*—the stellate cell plays a crucial role in transducing the diuretic kinin signal into a rapid increase in chloride conductance (8).

In practice, both transcellular and paracellular routes of chloride conductance are likely to contribute to both resting and kinin-stimulated fluid secretion (Fig. 1), but the relative importance of the two routes is not known. Here, we use *Drosophila* transgenics—combined with physiology, electrophysiology, and imaging—to show that a CLC chloride channel encoded by *ClC-a/CG31116* is a basolateral and apical plasma membrane chloride channel, uniquely localized to stellate cells, that is essential for neuropeptide-stimulated, but not resting, levels of secretion. Furthermore, by generating *Drosophila* that were transgenic for a membrane-targeted fluorescent chloride reporter, we demonstrate that tubule stellate cells displayed a characteristic intracellular chloride signature upon kinin stimulation. Therefore, we have resolved this issue in *Drosophila*; kinin stimulates chloride flux by a transcellular route that is confined to the stellate cells.

Significance

Endocrine control of chloride shunt conductance in Malpighian tubules of many insects is mediated by kinin diuretic peptides, but the route for chloride transport is unknown. We use *Drosophila* transgenics, combined with physiology, imaging, electrophysiology, and transgenic chloride reporter technology, to show that a chloride channel (CLC) encoded by *ClC-a/CG31116* is uniquely localized to stellate cells and is essential for neuropeptide-stimulated, but not resting, levels of secretion. Therefore, we have resolved this issue in *Drosophila*; kinin stimulates chloride flux by a transcellular route that is confined to the stellate cells.

Author contributions: P.C., S.T., S.A.D., E.M.B., and J.A.T.D. designed research; P.C., S.T., M.F.R., and E.M.B. performed research; P.C., S.T., S.A.D., E.M.B., and J.A.T.D. analyzed data; and P.C., S.T., S.A.D., E.M.B., and J.A.T.D. wrote the paper.

The authors declare no conflict of interest.

This article is a PNAS Direct Submission.

Freely available online through the PNAS open access option.

[1]P.C. and S.T. contributed equally to this work.

[2]To whom correspondence should be addressed. Email: julian.dow@glasgow.ac.uk.

This article contains supporting information online at www.pnas.org/lookup/suppl/doi:10.1073/pnas.1412706111/-/DCSupplemental.

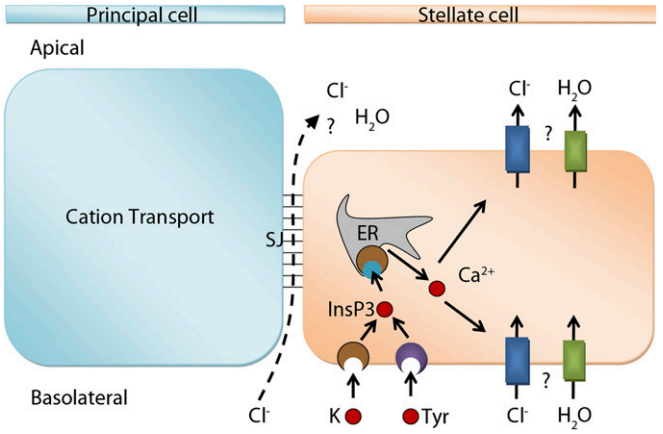

Fig. 1. Models for chloride flux. After kinin (K) or tyramine (Tyr) induction, chloride could take a paracellular route through septate junctions (SJ) or a transcellular route through yet-unidentified chloride channels in the stellate cells.

Results and Discussion

Two *CLC* Genes Show Enriched Expression in Tubules. Only two of the three *CLC* genes encoded by the *D. melanogaster* genome show highly abundant expression in adult Malpighian tubule (Fig. S1). By contrast, *ClC-b* shows low-level expression consistent with a predicted role as a housekeeping endomembrane channel. *Drosophila ClC-b* (*CG8594*) is a homolog of human *CLCN7* (*CLC-7*), an endosomal and lysosomal Cl^- channel that is thought to act as a $H^+/2Cl^-$ exchanger that provides the major chloride conductance of lysosomes (9, 10). Based on these distributions—and the functions of their respective homologs in humans—we focused our attention on the functional roles of *ClC-a* and *-c*.

Chloride Channel *ClC-a* Plays a Critical Role in Renal Function. *Drosophila ClC-a* (*CG31116*) is a homolog of human *CLCN2* (*CLC-2*), a plasma membrane inwardly rectifying chloride channel functionally significant in airway epithelia and the central nervous system. In epithelia, CLCN2 is apical and has been suggested to play a role in Cl^- efflux (11).

The GAL4/UAS binary expression system allows the knockdown of specific transcripts in specific cells within an otherwise normal organism, under control of the appropriate GAL4 driver lines. The Vienna UAS-dsRNA line *ClC-a*^{kk101247} produced a significant knockdown (>70%) in overall tubule expression of *ClC-a* when driven in stellate cells, but no knockdown when driven in principal cells (Fig. 2*A*), suggesting that *ClC-a* is expressed uniquely in the stellate cells.

ClC-a in only Stellate Cells Is Essential for Kinin-Induced Stimulation of Fluid Secretion. To determine whether *ClC-a* knockdown in stellate cells affected tubule physiology, we measured tubule secretion in control and *ClC-a* knockdown tubules (12). *ClC-a* RNAi knockdown in stellate cells had no effect on basal fluid secretion levels, but abolished the stimulation of fluid secretion normally induced by *Drosophila* kinin, a neuropeptide that activates the tubule chloride shunt pathway in *Drosophila* and other insects. By contrast, knockdown of *ClC-a* in principal cells had no effect on either resting or stimulated secretion. Therefore, *ClC-a* in stellate cells is essential for kinin-stimulated, but not resting, fluid secretion (Fig. 2 *B* and *C*).

Tubule Electrophysiology of Kinin-Induced Stimulation. Conceivably, *ClC-a* knockdown might have an impact indirectly on fluid secretion, rather than directly on chloride conductance. The electrophysiological signature of kinin action is a rapid abolition of the lumen-positive transepithelial potential difference (TEP), concomitant with an increase in fluid secretion, as the chloride conductance is rapidly increased. When kinin was applied to tubules in which *ClC-a* had been knocked down only in stellate cells, the change in electrical TEP was dramatically reduced. By contrast, knockdown in principal cells had no impact on the classical collapse in TEP/increase in fluid secretion signature (Fig. 2*D*). Therefore, kinin acts only in stellate cells to stimulate chloride conductance through *ClC-a*. By contrast, manipulations of *ClC-a* expression have absolutely no impact on the resting TEP or transport rates (Fig. S2), consistent with the lack of effect on basal secretion and implying that resting activity is maintained

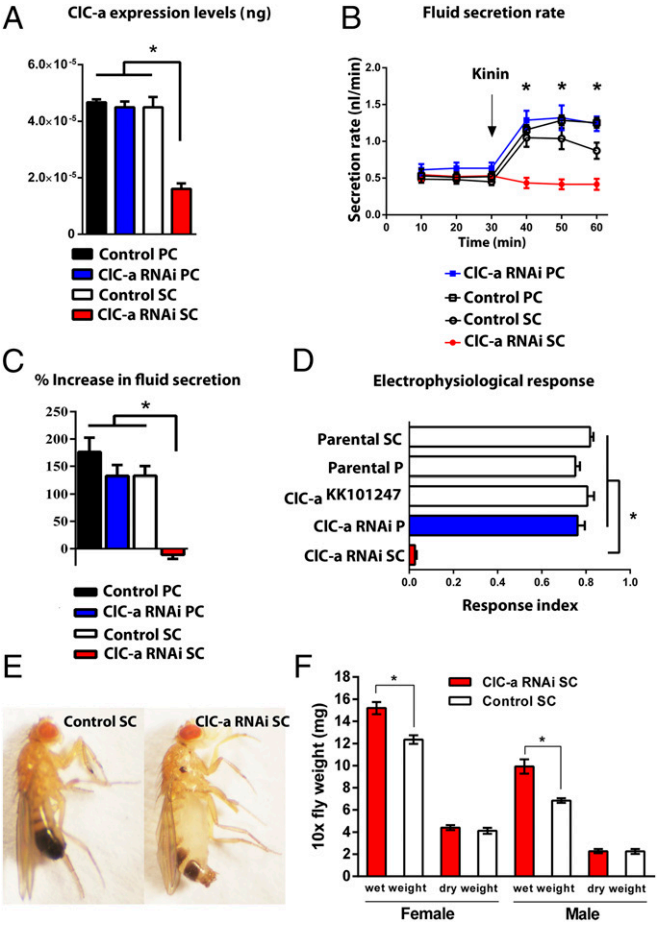

Fig. 2. Physiological and phenotypic effects of *ClC-a* down-regulation. (*A*) Cell-specific down-regulation of *ClC-a* in principal cells (PC) or stellate cells (SC) using the Vienna UAS-dsRNA line *ClC-a*^{kk101247}. Data are expressed as 10^{-5} ng of tubule *ClC* mRNA ± SEM ($n = 3$). *$P < 0.05$ (Student's *t* test). (*B*) Fluid secretion rates (nl·min^{-1}) in controls and *ClC-a* knockdown Malpighian tubules. *Drosophila* kinin (K) was added at 30 min (arrow). Response to 100 nM kinin is dramatically reduced in stellate-cell–specific *ClC-a* knockdown tubules (red). (*C*) Percentage increase from basal fluid secretion calculated from *B*. (*D*) Electrophysiological response index after K application in controls (white), *ClC-a* knockdown in principal cells (blue), and *ClC-a* knockdown in stellate cells (red). Response to K is abolished in stellate-cell–specific *ClC-a* knockdown tubules (red). (*E*) Control (*Left*) and *ClC-a* knockdown (*Right*) 1-wk-old male adults. *ClC-a* knockdown caused inflated abdomen phenotype. A similar phenotype is observed for females. (*F*) Wet- and dry-weight measurements for adults: male and female. Wet weight was significantly higher in *ClC-a* knockdown flies compared with controls. Data are expressed as mg ± SEM ($n \geq 3$, independent samples of 10 flies each in triplicate). *$P < 0.05$ [Student's *t* test (two-tailed)].

by a completely different route—for example, a paracellular conductance.

Bloated-Fly Phenotype. Stellate-cell–specific *ClC-a* knockdown also produced an inflated abdomen phenotype in adult flies, implying defective osmoregulation (Fig. 2*E*). To confirm that the abdominal bloating was due to increased haemolymph water content, we performed wet–dry weight measurements. Wet weight measurements revealed that *ClC-a* knockdown male and female adults are significantly heavier compared with control flies, whereas dry weight measurements are equivalent (Fig. 2*F*). Interestingly, the same distended abdomen phenotype was observed upon knockdown of *teashirt*, a transcription factor that regulates stellate cell differentiation and renal physiology in *Drosophila* (13).

Transients of $[Cl^-]_i$ in Stellate Cells During Kinin Receptor Activation. If kinin is indeed activating a stellate-cell–specific chloride shunt conductance, it may be possible to detect transient changes in intracellular chloride on kinin stimulation. To monitor stellate cell intracellular concentration of Cl^- ($[Cl^-]_i$), we made flies transgenic for a genetically encoded fluorescent combined Cl^-/pH -biosensor (ClopHensor) (14), under UAS control, allowing its cell-specific expression. The fluorescence of the PalmPalm-ClopHensor (Fig. 3*A*) confirms that that this transgenic sensor is typically localized to plasma and intracellular membranes, as seen in other systems (15, 16).

First, we measured the ratiometric changes in R_{Cl} *(F458/F545)* of the PalmPalm-ClopHensor, as described elsewhere (14), in response to application of 75 mM KCl to either single stellate cells (Fig. 3*B*) or individual Malpighian tubules (Fig. 3*C*), using confocal microscopy or spectrophotometer recording, respectively, to confirm the chloride sensitivity of the system.

Kinin stimulation in the tubule caused a strong increase of $[Cl^-]_i$ (Fig. 3*D*), likely due to chloride ion passage through the basolateral plasma membrane. After peaking, $[Cl^-]_i$ rapidly stabilized to values similar to normal, possibly due to partial desensitization of the kinin

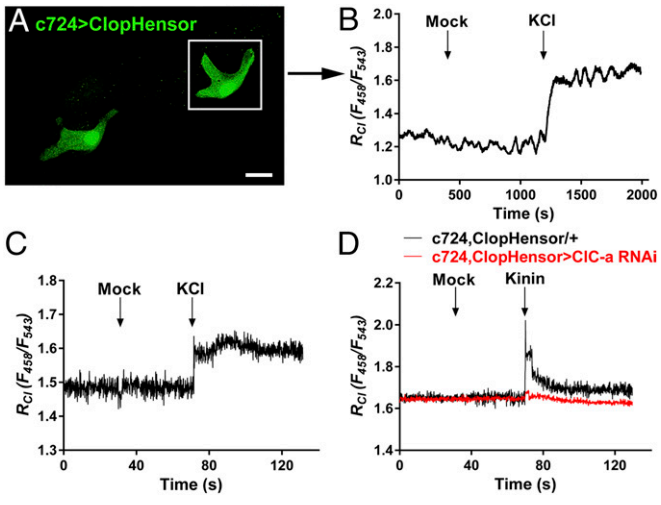

Fig. 3. Imaging and recording of PalmPalm-ClopHensor for chloride ions. (*A*) Merge of z-stack of the PalmPalm-ClopHensor chloride reporter, under UAS control and driven by c724 stellate-cell–specific GAL4 driver. (*B* and *C*) Single stellate cell imaging (*B*) and individual Malpighian tubule monitoring (*C*) of the PalmPalm-ClopHensor. Relative changes in *RCl (F458/F545)* of PalmPalm-ClopHensor measured in response to mock injection followed by application of 75 mM KCl. (*D*) Monitoring of transients of chloride ions during activation of *Drosophila* kinin receptor in control and *ClC-a* knockdown Malpighian tubules. The chloride response to *Drosophila* kinin (K; 10^{-7} M) is dramatically reduced in stellate-cell–specific *ClC-a* knockdown tubules (red).

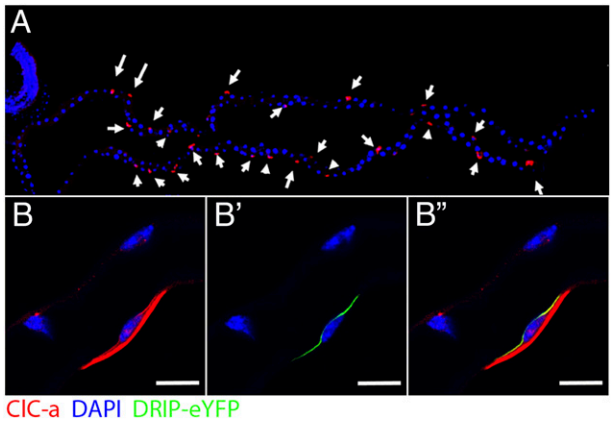

Fig. 4. Subcellular localization of CLC-a. (*A*) Antibody against CLC-a showed specific labeling of only stellate cells within the tubule (red, arrows), DAPI was used for nuclei staining (blue). (*B*) CLC-a (red) is expressed in both basolateral and apical membranes. (*B′*) Drip–eYFP was overexpressed specifically in stellate cells as an apical membrane marker. (*B″*) Colocalization (yellow) between Drip–eYFP and CLC-a in the apical membrane. (Scale bars: 10 μm.)

response and redistribution of chloride ions through the ClC-a chloride channel in the stellate cells or a transient mismatch between activation of basal and apical conductances. These changes were dramatically reduced in reporter lines in which *ClC-a* was specifically knocked down in only in tubule stellate cells, confirming that the changes seen were due to ClC-a chloride channel activation by kinin (Fig. 3*D*).

Where Is ClC-a Within the Cell? Real-time PCR data (Fig. 2*A*) show that *ClC-a* expression is primarily in the stellate cells, because only knockdown in stellate cells significantly impinges on overall tubule expression level. Although *ClC-a* is a homolog of a plasma-membrane chloride channel, and its knockdown leads to specific effects on transepithelial transport, it is conceivable that it could be an intracellular channel that in some way impinges indirectly on transepithelial chloride flux. Accordingly, it is important to establish where in the stellate cell it resides.

We raised a specific antibody against ClC-a and validated it by Western blotting (Fig. S3). Immunocytochemistry showed specific labeling of only stellate cells within the tubule (Fig. 4*A*), and confocal microscopy revealed that the location was on the plasma membrane (Fig. 4*B* and Fig. S4). By overexpressing in the stellate cell a known apical membrane aquaporin channel, Drip (17), labeled with enhanced YFP (eYFP) (Fig. 4*B′*), we were able to show that ClC-a both colocalizes apically with DRIP, and prominently labels the basal membrane. So although we cannot exclude additional chloride transport routes, ClC-a is present in both apical and basal plasma membranes and is both necessary and sufficient for kinin response (Fig. 4*B″*). Therefore, a plasma membrane ClC-a chloride channel, uniquely in the stellate cells, is essential for the action of kinin to stimulate fluid production by increasing the chloride conductance, so collapsing the transepithelial membrane potential.

We also were able to confirm by immunocytochemistry the efficiency of the knockdown of *ClC-a* expression at the protein level (Fig. 5). Only down-regulation of *ClC-a* in the stellate cell was able to replicate the effect of blocking the antibody with the antigenic peptide (Fig. 5*C*).

Chloride Channel *ClC-c* Does Not Play a Stellate-Specific Role. *ClC-a* is not the only chloride channel enriched in the tubule; *ClC-c (CG5284)*, a homolog of human *CLCN3* (*CLC-3*) known to play both plasma membrane and epithelial roles, is also tubule-enriched. In the plasma membrane of epithelia, it is implicated in

PHYSIOLOGY

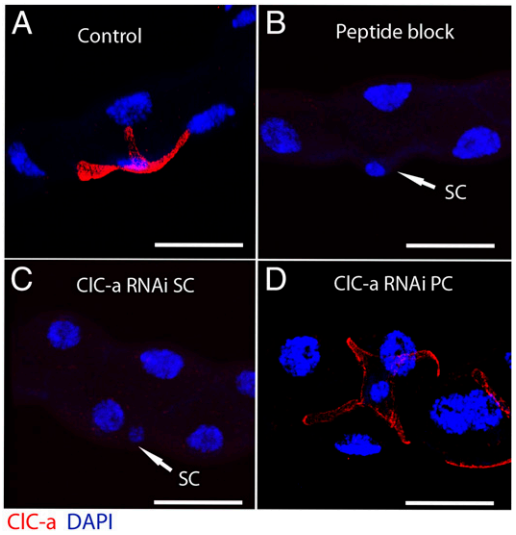

Fig. 5. Immunocytochemistry of ClC-a knockdown tubules. (*A*) Wild-type control tubule showing stellate cell localization of CLC-a. (*B*) Specificity was confirmed by blocking CLC-a antibody with the antigenic peptide. (*C*) Down-regulation of ClC-a in stellate cells (SC) abolishes CLC-a staining. (*D*) Knockdown of ClC-a in principal cells (PC) does not affect tubule CLC-a staining. (Scale bars: 25 μm.)

cell swelling (18–21). It is also strongly expressed in the nervous system, where it is found in endosomal compartments and synaptic vesicles; mice deficient for CLCN3 show gross neurological defects, such as blindness and loss of the hippocampus (21).

Accordingly, we performed the equivalent experiments on a knockdown of *ClC-c*. By contrast with *ClC-a*, knockdown of *ClC-c* in principal cells knocked down overall tubule *Clc-c* expression levels, whereas knockdown in stellate cells produced compensatory up-regulation of whole tubule expression, suggesting that *ClC-c* is expressed in both cell types and does not play a stellate-specific role (Fig. 6*A*). Similarly, fluid secretion was only partially reduced in stellate-specific *ClC-c* knockdown (Fig. 6 *B* and *C*). Significantly, electrophysiological analysis showed that knockdown of *ClC-c* in either principal or stellate cells did not have an impact on kinin-induced depolarization of the transepithelial potential (Fig. 6*D*), implying that *ClC-c* is not involved in the chloride shunt pathway, and so any impact on fluid secretion is through some other mechanism (for example, impaired lysosomal acidification). Consistent with the quantitative PCR (q-PCR) data, a specific antibody against ClC-c (Fig. S5), stained both principal and stellate cells uniformly (Fig. S6). Therefore, we conclude that, although *ClC-c* is important for tubule function, it is not a direct participant in transepithelial chloride ion transport.

Conclusion

The relative contributions of transcellular and paracellular flux and of specialized cell types in the integrated performance of an epithelium is a fundamental and important issue, in which experimental techniques have been limiting. By selecting the *Drosophila* as an experimental subject, powerful cell-type–specific transgenics provide valuable methodologies to address such questions. We have previously used cell-type–specific calcium reporters to show that the kinin-induced calcium signal is exclusively expressed in stellate cells, implying that they alone mediate the tissue response to kinin; here, we directly show that kinin actions on chloride flux—evidenced independently by increase in fluid secretion, increase in intracellular chloride, and decrease in transepithelial potential—all depend obligatorily on the presence of the plasma membrane chloride channel ClC-a. These results confirm the proposed spatial segregation of cation and anion transport in *Drosophila* into two distinct cell types (22, 23) and suggest that the paracellular pathway is more likely to account for basal, rather than kinin-stimulated, fluid secretion.

Although these transgenic technologies are not readily applied to other species, the model we have developed in *Drosophila* is likely to have more general application. In both the dengue vector *Aedes aegypti* (24), and the malaria vector *Anopheles gambiae* (25), kinin receptors have been localized to the stellate cells. Indeed, stellate cells are considered general to the Diptera. Excitingly, differentiated characters of the stellate role are under control of *teashirt* in *Drosophila*, and orthologs of *teashirt* have been found to be localized to previously undocumented secondary cells in highly diverged insect groups such as Orthoptera and Coleoptera (13). It may well be that the uniquely high secretory rates of many insect renal tubules can be explained by the model we show here.

Materials and Methods

Filtering of Candidate Chloride Channel Genes. Of the known chloride channel genes, members of the *ClC* gene family are obvious candidates for an epithelial function (26). In *Drosophila*, there are three such genes, and all are known to be expressed in tubules (27). The online resource FlyAtlas.org (28, 29) allows a more detailed view of gene expression across multiple tissues and life stages. Accordingly, FlyAtlas was interrogated for the full expression patterns of the three *Drosophila ClC* genes, to focus attention to those with likely epithelial roles.

***Drosophila* Stocks and Rearing.** *Drosophila* strains were reared at 22 °C, 45% relative humidity on a 12:12 photoperiod on standard *Drosophila* diet. Stocks

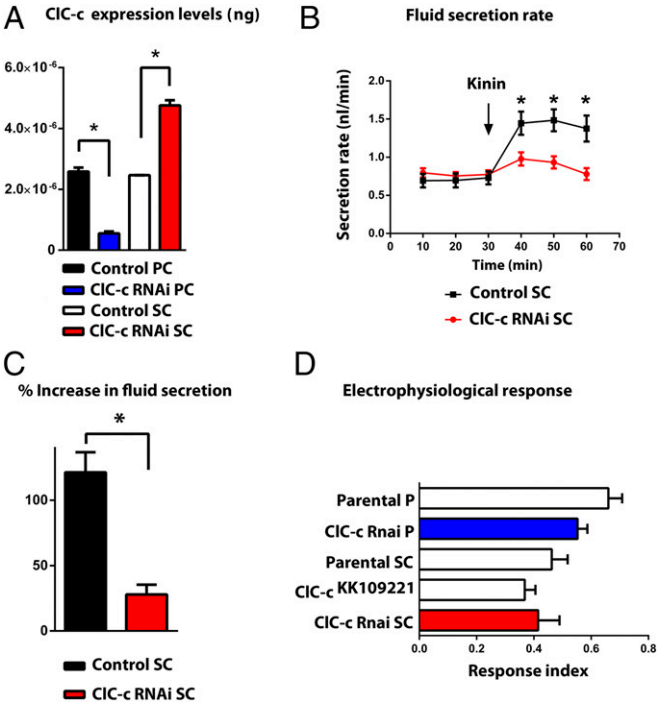

Fig. 6. Physiological effects of *ClC-c* down-regulation. (*A*) Cell-specific down-regulation of *ClC-c* in principal cells (PC) or stellate cells (SC) using the Vienna UAS-dsRNA line *ClC-c*^{kk109221}. (*B*) Fluid secretion rates (nL·min^{-1}) in control and *ClC-c* knockdown Malpighian tubules. *Drosophila* kinin (K) was added at 30 min (arrow). Response to 10^{-7} M kinin is reduced in stellate-cell–specific *ClC-c* knockdown tubules (red). (*C*) Percentage increase from basal fluid secretion calculated from *B*. (*D*) Electrophysiological response index after 5×10^{-8} M kinin application in controls (white) and *ClC-c* knockdown in principal cells (blue) and in stellate cells (red). Knockdown of *ClC-c* in either PC or SC did not have an impact on kinin-induced depolarization of the transepithelial potential compared with parental controls.

used were as follows: Canton-S, wild-type (Bloomington stock); c710/c710;$^{+/+}$ and w^{-};c724/c724;$^{+/+}$ GAL4 driver lines specific to stellate cells (30), used interchangeably in this study; w^{-};$^{+/+}$;c42/c42 and w^{-};uro-GAL4/uro-GAL4;$^{+/+}$, GAL4 drivers specific to principal cells, and used interchangeably in this study (30, 31); *ClC-a*^{KK101247}/*ClC-a*^{KK101247}, dsRNA line directed against *ClC-a* (Vienna stock V110394); *ClC-c*^{kk109221}/*ClC-c*^{kk109221} (Vienna stock 106844) and *ClC-c*^{JF02360}/*ClC-c*^{JF02360} (Bloomington stock 27034), dsRNA lines directed against *ClC-c*. P{UAS-DRIP-Venus} was generated as an apical membrane marker after induction with c724.w^{-};$^{+/+}$;P{UAS-Dcr-2.D}10 (Bloomington stock 24651) and w^{-}; P{UAS-Dcr-2.D}2;$^{+/+}$ (Bloomington stock 24650) were used to increase the efficiency of RNAi lines.

Validation of RNAi Knockdown. Knockdown of target genes relative to parental lines was assessed by quantitative RT-PCR (qRT-PCR). RNA was isolated from Malpighian tubules of 7- to 10-d-old flies by using the RNeasy kit (Invitrogen). cDNA was generated from 1 μg of RNA_T by using SuperScript II for each sample and q-PCR performed in Abgene One step plus real-time PCR. Taqman primers used were those commercially available from Abgene: Dm02148757_g1 (*ClC-a*), Dm01805573_g1 (*ClC-c*), and Dm02361072_s1 (*alpha tubulin 84B*). To evaluate the effect of down-regulation of *ClC-a* expression (Fig. 2*A*), the following lines were used: SC denotes stellate cell and PC principal cell: Control SC (w^{-}; *ClC-a*^{KK101247}/CyO; P{UAS-Dcr-2.D}10/TM2), *ClC-a* RNAi SC (w^{-}; *ClC-a*^{KK101247}/+; c710/P{UAS-Dcr-2.D}10), Control P (w^{-}; *CyO*/uro-Gal4;+/P{UAS-Dcr-2.D}10), *ClC-a* RNAi P (w^{-}; *ClC-a*^{KK101247}/uro-Gal4;+/P{UAS-Dcr-2.D}10). For *ClC-c* (Fig. 6*A*): Control SC (c724), *ClC-c* RNAi SC (w^{-}; *ClC-c*^{kk109221}/c724;$^{+/+}$), Control P (w^{-};uro-Gal4/+;$^{+/+}$), *ClC-c* RNAi PC (w^{-}; *ClC-c*^{kk109221}/uro-Gal4;$^{+/+}$).

Secretion Assays. Secretion assays were performed as described (12). Secretion rates were measured every 10 min; after 30 min of baseline readings, the diuretic peptide *Drosophila* kinin was added to 10^{-7} M, and secretion rates were measured for a further 30 min. At least seven tubules were used for each condition. The following lines were used: for *ClC-a* (Fig. 2 *B* and *C*), knockdown in stellate cells *ClC-a* RNAi SC (w^{-}; *ClC-a*^{KK101247}/+;c710/ P{UAS-Dcr-2.D}10) and principal cells *ClC-a* RNAi P (w^{-}; *ClC-a*^{KK101247}/uro-Gal4;+/P{UAS-Dcr-2.D}10) were compared with its control lines Control SC (w^{-}; *ClC-a*^{KK101247}/CyO;Tm2/P{UAS-Dcr-2.D}10 and Control PC (w^{-}; *CyO*/uro-Gal4;+/P{UAS-Dcr-2.D}10). For *ClC-c* (Fig. 6 *B* and *C*), knockdown in stellate cells *ClC-c* RNAi SC (w^{-}; *ClC-c*^{KK109221}/*c724*;$^{+/+}$) was compared with its control line Control SC (w^{-}; c724/c724;$^{+/+}$). Data are plotted as mean ± SEM. Where needed, data were compared by using the Student *t* test, taking $P = 0.05$ (two-tailed) as the critical value.

Fly Weight Measurements. To measure wet-body weight, groups of 10 male or female flies were anesthetized with CO_2, transferred to Eppendorf tubes on ice, and weighed on a AND GR-202 precision balance in triplicate. For dry-body weight, flies were killed by freezing for 20 min and subsequently dried at 60 °C for 24 h. Dry flies were weighed after reaching room temperature.

Electrophysiological Assays. Electrophysiological assays were performed as described (32); the TEP was measured with a sharp microelectrode with reference to the basolateral bath. The TEP depolarization upon treatment of tubules for 45 s with either 5×10^{-8} or 10^{-7} M *Drosophila* kinin (Anaspec) was quantified as a response index relative to control tubules, as described (33); For *ClC-a* RNAi knockdowns in stellate cells *ClC-a* RNAi SC (w^{-}; *ClC-a*^{KK101247}/P{UAS-Dcr-2.D}2;c710/+) and principal cells *ClC-a* RNAi P (w^{-}; *ClC-a*^{KK101247}/P{UAS-Dcr-2.D}2;c42/+) were compared with their parental lines, Parental SC (w^{-}; P{UAS-Dcr-2.D}2; c710), Parental P(w^{-}; P{UAS-Dcr-2.D}2; c42), and Parental *ClC-a*^{KK101247} (Fig. 2*D*). For *ClC-c,* again, RNA knockdowns in stellate cells *ClC-c* RNAi SC (w^{-}; *ClC-c*^{KK109221}/P{UAS-Dcr-2.D}2;c710/+) and Principal cells *ClC-c* RNAi P (w^{-}; *ClC-c*^{KK109221}/P{UAS-Dcr-2.D}2;c42/+) were compared with their parental lines, Parental SC (w^{-}; P{UAS-Dcr-2.D}2;c710), Parental P(w^{-}; P{UAS-Dcr-2.D}2;c42), and Parental *ClC-c*^{KK109221} (Fig. 6*D*).

Generation of Antibodies and Visualization of CLC Distribution. For CLC-a and -c, antigenic peptides in the deduced proteins were identified by using MacVector software. The peptides selected were as follows: CLC-a, QESKQSPSADKSNT; CLC-c, YEDFHTIDWQRDIAR. Polyclonal antisera were prepared and IgG-purified by Genosphere. The antibodies were further purified by using HiTrap NHS-Activated HP (Amersham Biosciences; catalog no. 17-0716-01). Specificity of antisera was established by Western blotting. Dissected Malpighian tubules were lysed in *Drosophila* lysis buffer (34) containing protease inhibitor mixture (Sigma-Aldrich) and sonicated. Using Novex Nupage 4-12 Bis-Tris Gel (NP0321BOX), electrophoresis of 20 μg per sample of lysate containing Nupage LDS sample Buffer was achieved following manufacturer's instructions and Nupage Mes SDS as running buffer. Blotting was performed by using a PVDF (Hybond P) membrane, Nupage Transfer Buffer (20×), NP0006-1, TBS-Tween 20 [TBST; TBS containing 0.1% (wt/vol) Tween 20 from Sigma-Aldrich], Blocking Buffer: TBS-Tween 20 containing 5% (wt/vol) nonfat miK powder; antibody buffer: TBS-Tween 20 containing 5% (wt/vol) BSA and 0.1% sodium azide; primary antibody: CLC-a or -c antibody 1 μg·mL^{-1} in antibody buffer. Secondary antibody was ECL anti-rabbit IgG (1:2,000) in antibody buffer. Western blot validations of antibody specificity are shown for CLC-a (Fig. S3) and CLC-c (Fig. S5).

Immunocytochemistry and confocal microscopy were performed as described (5). Briefly, whole-mount Malpighian tubules were fixed in 4% (wt/vol) paraformaldehyde for 20 min. After washes with PBS, tissues were permeabilized with PBST (PBS containing 0.1% Triton X-100; Sigma-Aldrich) and blocked with blocking solution [PBST+ 10% (vol/vol) Goat serum]. Antibodies were diluted in blocking solution (1:2,000 for CLC-a and 1:1,000 for CLC-c), and antigenic peptides were added to antibody solutions for controls "peptide block." Primary antibody incubations were performed overnight at 4 °C. Alexa Fluor 546-conjugated affinity-purified goat anti-rabbit antibody (Life Technologies; A-11035) was used at a dilution of 1:1,000 for visualization of the primary Polyclonal IgG and incubated overnight at 4 °C. After a series of washes with PBST and PBS, tubules were stained with 1 μg·mL^{-1} DAPI (Sigma-Aldrich) and mounted in vectashield (Vector Laboratories). Slides were viewed by using a Zeiss 510 META confocal microscope, and images were processed with a Zeiss LSM 5 Image Browser. Lines used were Canton-S for control staining (Figs. 4*A* and 5*A* and Figs. S4 and S6*A*) and peptide block (Figs. 4*B*, 5*B*, and 6*B* and Fig. S6*B*); *ClC-a* RNAi SC, w^{-}; *ClC-a*^{KK101247}/+;c710/P{UAS-Dcr-2.D}10 (Fig. 6*C*); *ClC-a* RNAi PC, w^{-}; *ClC-a*^{KK101247}/uro-Gal4;+/P{UAS-Dcr-2.D}10 (Fig. 5*D*); *ClC-c* RNAi SC, w^{-};c724/+; *CLC-c*^{JF02360}/+ (Fig. S6*C*); *ClC-c* RNAi P, w^{-};uro-Gal4/+; *CLC-c*^{JF02360}/+ (Fig. S6*D*) and w^{-};c724/P{UAS-DRIP-Venus};$^{+/+}$ (Fig. 4 *B* and *B″*).

Generation of P{UAS-Drip-Venus} and P{UAS-PalmPalm-ClopHensor} Transgenic *Drosophila* Lines. The coding sequence of *Drosophila Drip* gene (*CG9023*) was amplified by PCR using DreamTaq green PCR master mix (Thermo Scientific) using the following primers: forward, CACCATGGTCGAGAAAACAGA; reverse, GAAGTCGTACGAGTCGGTCTC. The product was cloned into pENTR donor vector (Invitrogen) and transferred to pTWV destination vector (DGRC) by using Gateway LR Clonase II Enzyme mix according to the manufacturer's instructions. For amplification of the chloride reporter PalmPalm-ClopHensor (14), pcDNA3-PalmPalm-ClopHensor (Addgene plasmid 25940) was used as a template. The primers were forward, CACCATGAGCAAGGGCGA; and reverse, CTACTGGGAGCCGGACTGG. The product was cloned into pENTR donor vector (Invitrogen) and transferred to pTW destination vector (DGRC). The sequence integrity for each construct was confirmed by GATC Biotech, and transgenic lines were generated by using standard methods for P-element–mediated germ-line transformation (BestGene).

Measurement of Chloride Levels. For real-time chloride-ion imaging, individual Malpighian tubules from 7-d-old adult progeny of a c724 > UAS-PalmPalm-ClopHensor cross were stuck (in PBS) to the bottom of a glass-bottomed dish that had been treated with poly-L-lysine. Once the tubules were attached, the PBS was immediately removed, and 3 mL of Schneider's solution was added. The samples were left for at least 1 h before imaging, to allow the tubules to recover from any stimuli that might have occurred within the fly before dissection. Transgenic tubules expressing the reporter were imaged on a Zeiss 510 metaconfocal system coupled to an inverted Zeiss microscope. The ClopHensor reporter was excited at 458 nm for Cl^{-}-sensitive E^2GFP excitation and 545 nm for excitation of DsRed-monomer. Fluorescent signals were recorded by using two emission filters: 535 ± 15 nm for E^2GFP emission and 630 ± 30 nm for emission of DsRed-monomer. Real-time images of the tubule-expressing ClopHensor were captured, and fluorescence for single stellate cell was determined.

For Malpighian tubule monitoring of the PalmPalm-ClopHensor, tubules were placed in 185 μL of Schneider's medium in a well of a UV-transparent polystyrene 96-well plate (Berthold Technologies). Fluorescence recordings (as described above) were performed by using a Mithras LB940 automated 96-well plate reader (Berthold Technologies) and MikroWin software. A total of 15 μL of kinin was applied to a final concentration of 10^{-7} M. Because ClopHensor is an inverse reporter, the fluorescence values obtained were subtracted from a higher arbitrary value to convert fluorescence decrease to chloride level increase over time.

Statistics. Data are plotted as mean ± SEM. Where needed data were compared using Student *t* test, taking $P = 0.05$ (two-tailed) as the critical value. Where more than one group is compared with an experimental group, the highest *P* value is shown.

ACKNOWLEDGMENTS. This work was supported by Biotechnology and Biological Sciences Research Council Grants BB/G020620/1 and BB/L002647/1 and National Institutes of Health Grants DK092408 and DK100227.

1. Skaer HlB, Maddrell SHP (1987) How are invertebrate epithelia made tight? *J Cell Sci* 88:139–141.
2. Beyenbach KW, Baumgart S, Lau K, Piermarini PM, Zhang S (2009) Signaling to the apical membrane and to the paracellular pathway: Changes in the cytosolic proteome of *Aedes* Malpighian tubules. *J Exp Biol* 212(Pt 3):329–340.
3. Beyenbach KW (2003) Regulation of tight junction permeability with switch-like speed. *Curr Opin Nephrol Hypertens* 12(5):543–550.
4. Terhzaz S, et al. (1999) Isolation and characterization of a leucokinin-like peptide of Drosophila melanogaster. *J Exp Biol* 202(Pt 24):3667–3676.
5. Radford JC, Davies SA, Dow JAT (2002) Systematic G-protein-coupled receptor analysis in Drosophila melanogaster identifies a leucokinin receptor with novel roles. *J Biol Chem* 277(41):38810–38817.
6. Cabrero P, Richmond L, Nitabach M, Davies SA, Dow JAT (2013) A biogenic amine and a neuropeptide act identically: Tyramine signals through calcium in Drosophila tubule stellate cells. *Proc Biol Sci* 280(1757):20122943.
7. Blumenthal EM (2003) Regulation of chloride permeability by endogenously produced tyramine in the Drosophila Malpighian tubule. *Am J Physiol Cell Physiol* 284(3): C718–C728.
8. Dow JAT (2012) The versatile stellate cell - more than just a space-filler. *J Insect Physiol* 58(4):467–472.
9. Graves AR, Curran PK, Smith CL, Mindell JA (2008) The Cl-/H+ antiporter ClC-7 is the primary chloride permeation pathway in lysosomes. *Nature* 453(7196):788–792.
10. Leisle L, Ludwig CF, Wagner FA, Jentsch TJ, Stauber T (2011) ClC-7 is a slowly voltage-gated 2Cl(-)/1H(+)-exchanger and requires Ostm1 for transport activity. *EMBO J* 30(11):2140–2152.
11. Schiffhauer ES, et al. (2013) Dual activation of CFTR and CLCN2 by lubiprostone in murine nasal epithelia. *Am J Physiol Lung Cell Mol Physiol* 304(5):L324–L331.
12. Dow JAT, et al. (1994) The malpighian tubules of *Drosophila melanogaster:* A novel phenotype for studies of fluid secretion and its control. *J Exp Biol* 197:421–428.
13. Denholm B, et al. (2013) The tiptop/teashirt genes regulate cell differentiation and renal physiology in Drosophila. *Development* 140(5):1100–1110.
14. Arosio D, et al. (2010) Simultaneous intracellular chloride and pH measurements using a GFP-based sensor. *Nat Methods* 7(7):516–518.
15. McCabe JB, Berthiaume LG (1999) Functional roles for fatty acylated amino-terminal domains in subcellular localization. *Mol Biol Cell* 10(11):3771–3786.
16. Mukhtarov M, et al. (2013) Calibration and functional analysis of three genetically encoded Cl(-)/pH sensors. *Front Mol Neurosci* 6:9.
17. Kaufmann N, et al. (2005) Developmental expression and biophysical characterization of a Drosophila melanogaster aquaporin. *Am J Physiol Cell Physiol* 289(2):C397–C407.
18. Guzman RE, Grieschat M, Fahlke C, Alekov AK (2013) ClC-3 is an intracellular chloride/proton exchanger with large voltage-dependent nonlinear capacitance. *ACS Chem Neurosci* 4(6):994–1003.
19. Huang P, et al. (2001) Regulation of human CLC-3 channels by multifunctional Ca2+/calmodulin-dependent protein kinase. *J Biol Chem* 276(23):20093–20100.
20. Remillard CV, Yuan JX (2005) ClC-3: More than just a volume-sensitive Cl- channel. *Br J Pharmacol* 145(1):1–2.
21. Stobrawa SM, et al. (2001) Disruption of ClC-3, a chloride channel expressed on synaptic vesicles, leads to a loss of the hippocampus. *Neuron* 29(1):185–196.
22. O'Donnell MJ, Dow JAT, Huesmann GR, Tublitz NJ, Maddrell SHP (1996) Separate control of anion and cation transport in malpighian tubules of *Drosophila Melanogaster*. *J Exp Biol* 199(Pt 5):1163–1175.
23. O'Donnell MJ, et al. (1998) Hormonally controlled chloride movement across *Drosophila* tubules is via ion channels in stellate cells. *Am J Physiol* 274(4 Pt 2):R1039–R1049.
24. Lu HL, Kersch C, Pietrantonio PV (2011) The kinin receptor is expressed in the Malpighian tubule stellate cells in the mosquito Aedes aegypti (L.): A new model needed to explain ion transport? *Insect Biochem Mol Biol* 41(2):135–140.
25. Radford JC, Terhzaz S, Cabrero P, Davies SA, Dow JAT (2004) Functional characterisation of the Anopheles leucokinins and their cognate G-protein coupled receptor. *J Exp Biol* 207(Pt 26):4573–4586.
26. Jentsch TJ, Friedrich T, Schriever A, Yamada H (1999) The CLC chloride channel family. *Pflugers Arch* 437(6):783–795.
27. Chintapalli VR, Wang J, Herzyk P, Davies SA, Dow JAT (2013) Data-mining the FlyAtlas online resource to identify core functional motifs across transporting epithelia. *BMC Genomics* 14:518.
28. Chintapalli VR, Wang J, Dow JAT (2007) Using FlyAtlas to identify better Drosophila melanogaster models of human disease. *Nat Genet* 39(6):715–720.
29. Robinson SW, Herzyk P, Dow JAT, Leader DP (2013) FlyAtlas: Database of gene expression in the tissues of *Drosophila melanogaster*. *Nucleic Acids Res* 41(Database issue, D1):D744–D750.
30. Sözen MA, Armstrong JD, Yang M, Kaiser K, Dow JAT (1997) Functional domains are specified to single-cell resolution in a *Drosophila* epithelium. *Proc Natl Acad Sci USA* 94(10):5207–5212.
31. Terhzaz S, et al. (2010) Cell-specific inositol 1,4,5 trisphosphate 3-kinase mediates epithelial cell apoptosis in response to oxidative stress in Drosophila. *Cell Signal* 22(5): 737–748.
32. Blumenthal EM (2001) Characterization of transepithelial potential oscillations in the Drosophila Malpighian tubule. *J Exp Biol* 204(Pt 17):3075–3084.
33. Blumenthal EM (2009) Isoform- and cell-specific function of tyrosine decarboxylase in the Drosophila Malpighian tubule. *J Exp Biol* 212(Pt 23):3802–3809.
34. Sullivan W, Ashburner M, Hawley RS, eds (2000) Drosophila *Protocols* (Cold Spring Harbor Laboratory, Cold Spring Harbor, NY), pp 563–569.